論 文
35~12~4

유한요소법에 의한 2자유도 스텝모터의 설계

Design of Prototype Rotary-Linear Step Motor by the Finite Element Method

鄭 泰 庚* · 韓 松 曄** · 元 鍾 洙**

(Tae- Kyung Chung · Song- Yop Hahn · Jong - Soo Won)

요 약

본 논문에서는 로버트의 팔, NC 기계등에 이용될 수 있는 새로운 형태의 2자유도 스텝모터를 설계 제작하였다. 2자유도 스텝모터(Rotary-Linear Step Motor, RLSM)는 로터의 축이 회전운동과 직선운동을 동시에 할 수 있도록 설계하였다. 일반적으로 스텝모터는 공극이 매우 작아서 동작점에서 teeth 부분이 포화되므로 정확한 토오크와 force(推力), 인덕턴스를 구하기 위하여 비선형 유한요소법을 이용하였으며 실제제작하여 특성을 검토하였다.

Abstract

In this paper, a new type of step motor with two degree of mechanical freedom, which is named Rotary–Linear Step Motor(RLSM), is presented. Its rotor axis can perform linear and rotary motions either separately or simultaneously.

This paper discribes the design of RLSM using finite element method in which the magnetic saturation effect of the iron core is taken into account. The design parameters such as torques, forces and inductances are obtained from the computed magnetic vector potentials.

A new type of Rotary–Linear Step Motor was constructed. The calculated parameters agree well with measurements.

1. Introduction

Step motors with one degree of mechanical freedom are generally used for incremental motion control systems. To obtain more complicated motion often needed in industry(e.g. machine tools, robot arms), two or more step motors with appropriate mechanical interface are usually used.

In this paper, a new type of step motor with two degrees of mechanical freedom, which is named Rotary–Linear Step Motor(RLSM), is presented. Its rotor axis can perform linear and rotary motions either separately or simultaneously. A schematic diagram of RLSM is shown in Figure 1. The RLSM has a double air gap structure of which the outside has an ordinary multistack VR step motor with axial teeth of the stator and the rotor, and whose inside is similar to that of a tubular linear step motor with circumferential teeth of the stator and the rotor. Therefore the cylindrical holl-
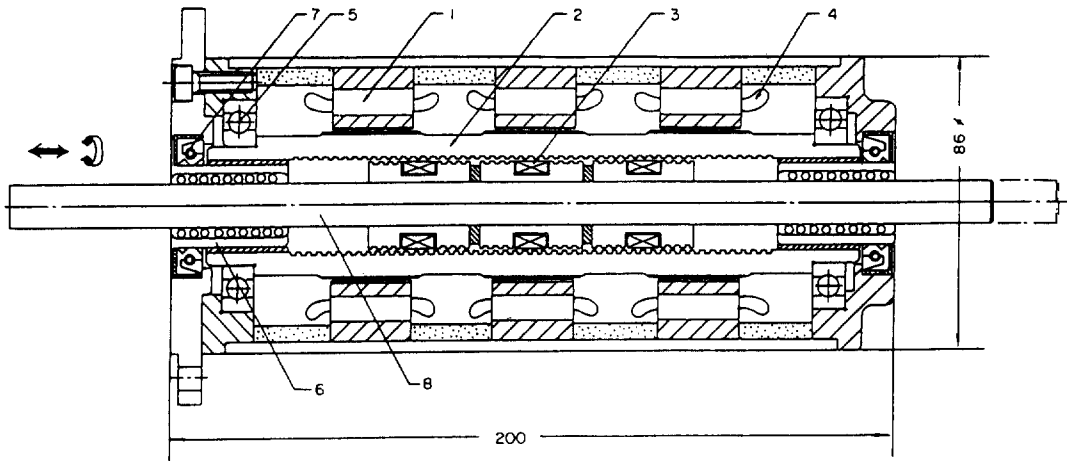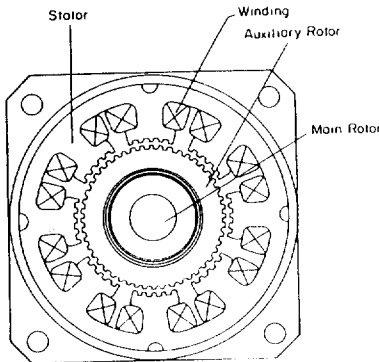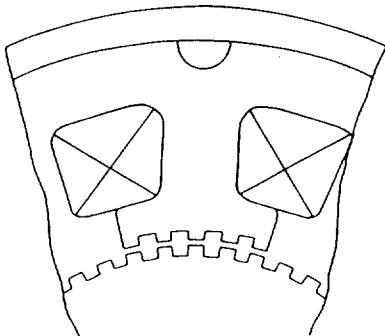
1. stator core of rotary motion region   2. auxiliary rotor   3. winding of linear motion region

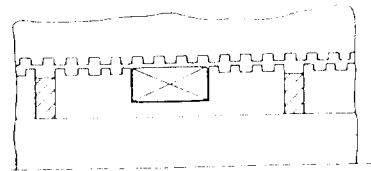4. stator winding 5. rotary bearing   6. linear bearing   7. oil seal   8. main rotor axis

Fig.1(a). Schematic diagram of RLSM structure.

Fig.1(b). Cross sectional view of RLSM

Fig.1(c). Detailed sketch of rotary motion region

Fig.1(d). Detailed sketch of linear motion region.

owshaped auxiliary rotor between air gaps is used as not only the rotor of the rotary motion region but the stator of the linear motion region. These three iron parts are combined with the rotary and linear bearings. The unique feature of the RLSM is such that the rotary motion and linear motion can be controlled independently.

This paper describes the computer–aided design of RLSM using finite element method in which the magnetic saturation effect of the iron core is taken into account. The design parameters such as torques, forces and inductances are obtained from the computed magnetic vector potentials. Applying the finite element method, the rotary motion region of RLSM is modeled using two dimensional planar finite elements with current and vector potential axially directed (z–direction), and its linear motion region is modeled using axi-symmetric finite elements with current and vector potential circumferentially directed(θ –direction).

2. Finite Element Method

The finite element method has been applied to analysis and design of electromagnetic devices[1),2)] Especially, the method is powerful to deal with complicated geometries made of nonlinear or conducting materials.

The finite element method is based on energy conservation. The law of conservation of energy in electromagnetic field systems may be derived from Maxwell's equations[3)]. The variational techniques such as the finite element obtain solutions to field problems by minimizing an energy functional. The functional is expressed by the difference between the stored energy and the input energy in the system volume[4)], viz.,

$$\pi = \int_V \left[\int_0^B \overline{H} \cdot d\overline{B} - \int_0^A \overline{J} \cdot d\overline{A} \right] dV \qquad (1)$$

where $\overline{B}$, $\overline{H}$, $\overline{A}$, and $\overline{J}$ are the magnetic flux density, magnetic field intensity, magnetic vector potential and current density, respectively. π is minimized when :

$$\frac{\partial \pi}{\partial A} = 0 \qquad (2)$$

Equation(2) finally leads to a set of simultaneous nonlinear equations,

$$[S]\{A\} = \{T\} \qquad (3)$$

where the matrix[S] represents the shape and physical properties of the materials.

Newton-Raphson Algorithm

The system matrix equation described in Eq.(3) is in general nonlinear due to saturable materials. To deal with this nonlinearity, the Newton-Raphson method is applied. Since the permeability of the iron core is not constant, the matrix[S] depends on the magnitude of $\overline{B}$ and $\overline{J}$. An iterative procedure is developed by expanding Eq.(2) in a multidimensional Taylor's series.

$$\frac{\partial \pi}{\partial A_i}\bigg|_{A+\delta A} = \frac{\partial \pi}{\partial A_i}\bigg| - \sum \frac{\partial^2 \pi}{\partial A_i \partial A_j}\bigg|_{A+\delta A} \cdot \delta A_j + \cdots \quad (4)$$

where i and j are integers varying from 1 to N.

Substitution Eq.(4) into Eq.(2) gives the following matrix equation[4)]

$$\delta A_j = - \left| \frac{\partial^2 \pi}{\partial A_i \partial A_j} \right|^{-1}_{A+\delta A} \cdot \frac{\partial \pi}{\partial A_i}\bigg|_{A+\delta A} \qquad (5)$$

This equation is the basis of Newton-Raphson algorithm used to solve for $\overline{A}$ in a saturable magnetic field. The Jacobian matrix in Eq.(5) is first estimated from an initial solution using approximate materials permeabilities. Then Eq.(5) is solved iteratively until the correction of A_j is negligibly small. In each solution of Eq.(5), both the Jacobian matrix and the residual vector in its right hand side are re-evaluated based on the latest A values, ensuring rapid convergence to correct saturable potentials $\overline{A}$ throughout the device.

The exact expressions for the Jacobian matrix and residual vector of Eq.(5) are derived elsewhere for planar[7)] and for axisymmetric[5)] problems. The technique requires knowledge of reluctivity $\nu(=1/\mu)$ and of $\partial\nu/\partial(B^2)$ in each nonlinear material. Here, these parameters are automatically computed from the B-H curves supplied as input data.

3. Postprocessing to Obtain Design Parameters

While the distribution of magnetic vector potential $\overline{A}$ obtained above has little meaning to design engineers, many useful parameters can be calculated from $\overline{A}$.

The flux density $\overline{B}$ is calculated in each finite element using the equation as defined in Eq.(6).

$$\overline{B} = \nabla \times \overline{A} \qquad (6)$$

Also, flux plots are obtained and displayed, which tell the designer where steel should be added and where it can be removed.

Force and Torque Calculations

The force and torque are obtained by the surface integrations of a surface stress $\overline{P}$ over an air gap enclosing the rotor body[6)], i.e.:

$$\overline{F} = \int_V \overline{f}dv = \oint_s \overline{p}ds \qquad (7)$$

$$\overline{T} = \int_V \overline{r} \times \overline{f}dv = \oint_s \overline{r} \times \overline{p}ds \qquad (8)$$

The exact expression of stress $\bar{P}$ is given by Eq.(9).

$$\bar{P} = \frac{1}{\mu_0}(\hat{n} \cdot \bar{B})\bar{B} - \frac{1}{2\mu_0}B^2\hat{n} \tag{9}$$

where n is the unit vector normal to the integration path. It is noted that in above expressions, the nonlinear characteristic of the body which is enclosed by the surface s is not directely expressed. The procedure of the calculation of force $\bar{F}$ and torque $\bar{T}$ by means of Eqs.(7) and (8) is as follows: — Calculate the vector potentials using finite element method.

— Define the integration surface s along the air gap. Any s should result in the same force and torque as long as the rotor body is fully enclosed.

— Calculated $\bar{B}$ by means of Eq.(6).

— Calculate the surface stress Pᵢ of Eq.(9) in each element.

— Calculate the force $\bar{F}$ and the torque $\bar{T}$:

$$\bar{F} = \sum \triangle \bar{F}_i = \sum \bar{P}_i \cdot \triangle A_i \tag{10}$$

$$\bar{T} = \sum \triangle \bar{T}_i = \sum \bar{r}_i \times \bar{p}_i \cdot \triangle A_i \tag{11}$$

Inductance

From vector potential $\bar{A}$, the saturable inductances L seen by each current carrying coil can be calculated for magnetic problems as follows:

$$L \cdot 1 = N \int \bar{B} \cdot d\bar{s}$$
$$= N \int \nabla \times \bar{A} d\bar{s}$$
$$= N \oint \bar{A} \cdot d\bar{l}$$
$$= \sum A^e \cdot N \cdot S_e \cdot 1 \tag{12}$$

where S_e is the area of triangular element, I is the coil current, N is the number of turns per unit area, l is the length of the number of turns stator stack, and A^e is the vector potential of the center of the triangular element.

4. Application to Rotary–Linear Step Motor

The Rotary–Linear Step motor is shown in Figure 1. It consists of three–stack stator, auxiliary rotor, and three–phase main rotor with ring–type coils. The two air gaps are maintained by rotary and linear bearings respectively. The main rotor coils are connected to outside driver through the rotor axis. This umbilical cord problem confines the rotary motion only to two or three revolutions.

Two dimensional model of the rotary motion region is shown is Figure 2. By applying the periodic boundary conditions to the two radial boundaries of the model, only one pole (45°) is required for modelling. Figure 3 shows the saturable flux
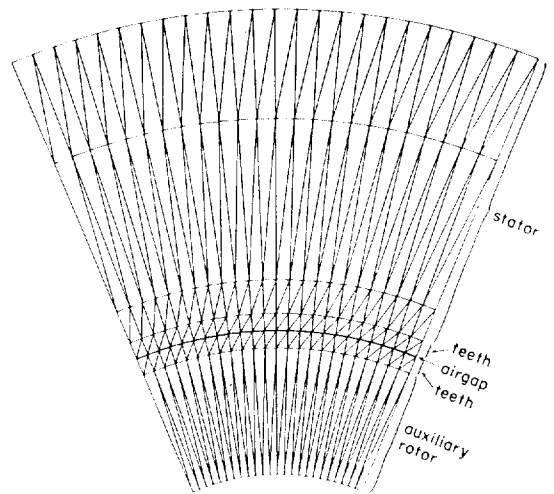

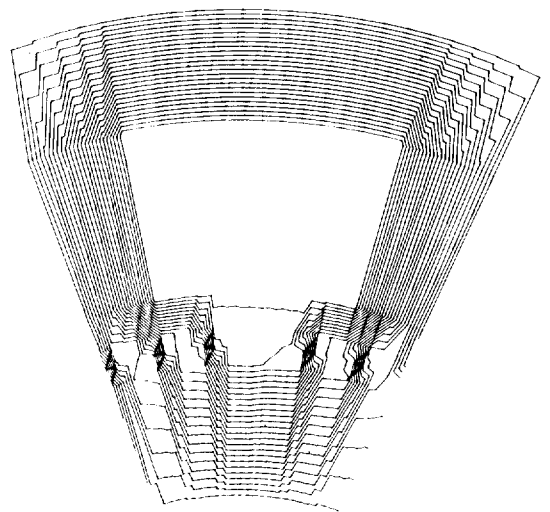**Fig.2.** Finite element model of rotary motion region.

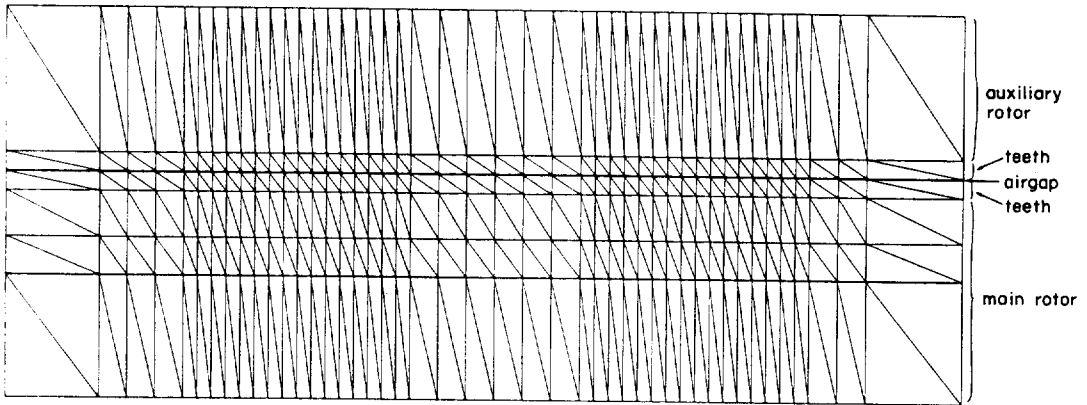**Fig.3.** Saturable flux plot for model of Fig.2.

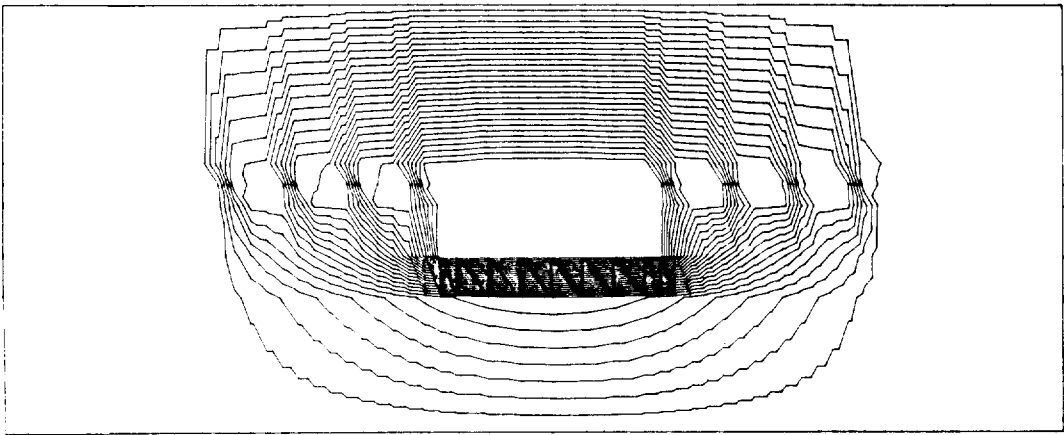**Fig.4.** Axisymmetric finite element model of linear motion region.

Fig.5. Saturable flux plot for model of Fig.4.

plot for the madel in Figure 2. The axisymmetric finite element model of the one phase of the linear motion region is shown in Figure 4. And its saturable flux pattern is shown in Figure 5 associated with the homogeneous boundary conditions.

5. Test and Result

To investigate the performance of the RLSM, and validity of the design parameters found numericelly, the prototype of RLSM depicted in Figure 8 has been built with the following characteristics :
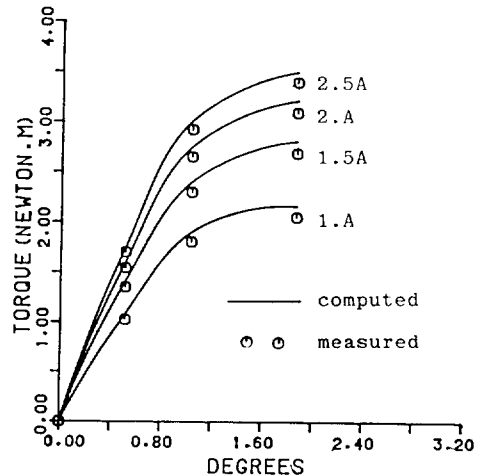
Rotary motion region :

Fig.6 Holding torques with rotor position.

stator length	25 mm
stator outer diameter	80 mm
stator inner diameter	43.5 mm
airgap length	0.05 mm
number of turns per pole	90 turns
number of teeth	48
step angle	2.5 degrees / pulse

Linear motion region :

main rotor diameter	27 mm
main rotor length per phase	31.3 mm
number of turns per phase	210 turns
airgap length	0.05 mm
step size	1 mm/pulse
stroke	50 mm

In figures 6 and 7, the forces and torques versus rotor position and current are shown.

The calculated holding torques and forces of the RLSM agree with the measured values within 5%.
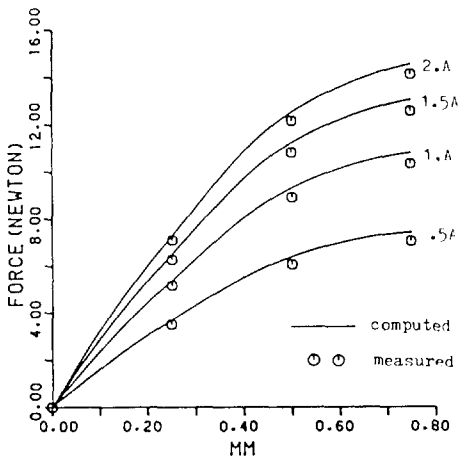

Fig.7. Axial forces with rotor position.

Fig.8. Prototype of rotary-linear step motor.

The resulting calculated peak magnetic flux density of rotor is 2.1 T. The saturable inductances of stator and rotor found numerically are max. 118 mH, min. 44 mH and max. 83 mH, min. 34 mH, at current 2A respectively.

6. Conclusion

A new type of Rotary–Linear Step Motor was proposed and constructed. Finite Element Method was applied to calculate parameters of the RLSM. Torques and forces are found using the surface integration of the magnetic stress along the air gap. Finite element method is shown to be a good design tool of electromagnetic devices. The calculated parameters agree well with measurements. This work was supported by Das Woo Heavy Industries, Ltd.

References

1) P.Silvester and M.V.K. Chari, "Finite Element Solution of Saturable Magnetic Field Problems", IEEE Trans. on PAS, Vol. PAS–89, No. 7, pp.1642–1652, Sept./Oct. 1970.

2) Parviz Rafinejad and J.C.Sabonnadiere, "Finite Element Computer Programs in Design of Electromagnetic Devices", IEEE Trans. on MAG., Vol. MAG–12, No.5, Sept. 1976.

3) W.K.H. Panofsky and M.Phillips, Classical Electricity and Magnetism, Addison–Wesley Publishing Company, INC., 1964.

4) P.Silvester, H.S. Cabayan, and B.T.Browne, "Efficient Techniques for Finite–Element Analysis of Electric Machine", IEEE Trans. on PAS, Vol. PAS–92, pp.1274–1281, 1973.

5) Eric Munro, "Some Techniques of the Finite Element Method for solving Magnetic Field Problems", Proceedings on COMPUMAG, pp.35–45, 1976.

6) K.Reichert, H.Freundl, and W.Vogt, "The Calculation of Force and Torques within Numerical Magnetic Field Calculation Methods", Proceedings on COMPUMAG, pp.64–73, 1976.

7) T.Nakata and N.Takahashi: Finite Element Method in Electrical Engineering (book in Japanese), Morikita shuppan, Tokyo, 1982.